Special Topics & Reviews in Porous Media — An International Journal, 5 (1): 27–39 (2014)

VISCOUS DISSIPATION AND MAGNETIC FIELD EFFECTS IN A NON-DARCY POROUS MEDIUM SATURATED WITH A NANOFLUID UNDER CONVECTIVE BOUNDARY CONDITION

A. J. Chamkha,[1] A. M. Rashad,[2,*] Ch. RamReddy,[3] & P. V. S. N. Murthy[4]

[1]*Manufacturing Engineering Department, Public Authority for Applied Education and Training, Shuweikh, 70654, Kuwait*

[2]*Department of Mathematics, Aswan University, Faculty of Science, 81528, Egypt*

[3]*Department of Mathematics, National Institute of Technology Warangal-506004, India*

[4]*Department of Mathematics, Indian Institute of Technology, Kharagpur-721 302, India*

[*]Address all correspondence to A. M. Rashad E-mail: am_rashad@yahoo.com

Original Manuscript Submitted: 2/28/2013; Final Draft Received: 12/4/2013

This paper investigates the influence of viscous dissipation and magnetic field on natural convection from a vertical plate in a non-Darcy porous medium saturated with a nanofluid. In addition, a convective boundary condition is incorporated in the nanofluid model. A nonsimilarity transformation is used to reduce the mass, momentum, thermal energy, and the nanoparticle concentration equations into a set of nonlinear partial differential equations. The obtained equations are solved numerically by an accurate implicit finite-difference method. The accuracy of the numerical results is validated by a quantitative comparison of the heat transfer rates with previously published results for a special case and the results are found to be in good agreement. The effects of magnetic field, viscous dissipation, and non-Darcy and the convection parameters on the velocity, temperature, nanoparticle volume fraction, and heat and nanoparticle mass transfer rates are illustrated graphically.

KEY WORDS: *free convection, non-Darcy, nanofluid, magneto-hydrodynamics, viscous dissipation, convective boundary condition*

1. INTRODUCTION

In recent years, the flow analysis of nanofluids has been the topic of extensive research due to its characteristic in increasing thermal conductivity in heat transfer process. Several ordinary fluids, including water, toluene, ethylene glycol, and mineral oils, etc., in heat transfer processes have rather low thermal conductivity. The nanofluid [initially introduced by Choi (1995)] is an advanced type of fluid containing nanometer-sized particles (diameter less than 100 nm) or fibers suspended in the ordinary fluid. Undoubtedly, the nanofluids are advantageous in the sense that they are more stable and have acceptable viscosity and better wetting, spreading, and dispersion properties on solid surfaces. Nanofluids are used in different engineering applications such as microelectronics, microfluidics, transportation, biomedical, solid-state lighting, and manufacturing. In particular, nanofluids are suspensions of nanoparticles in fluids that show significant enhancement of their properties at modest nanoparticle concentrations. Nanofluids have been demonstrated to be able to handle this role in some instances as a smart fluid. The research on heat transfer in nanofluids has been receiving increased attention worldwide. Many researchers

2151–4798/14/$35.00

have found unexpected thermal properties of nanofluids, and have proposed new mechanisms behind the enhanced thermal properties of nanofluids. For details and methodologies of convective heat transfer in nanofluids, the reader is referred to the book by Das et al. (2007) and in the review papers by Buongiorno (2006) and Kakac and Pramuanjaroenkij (2009).

In view of these applications, many researchers have begun research in this field. Nield and Kuznetsov (2009a,b) analyzed the free convective boundary layer flows in a porous medium saturated by nanofluid by taking Brownian motion and thermophoresis effects into consideration. Chamkha et al. (2011) carried out a boundary layer analysis for the natural convection past an isothermal sphere in a Darcy porous medium saturated with a nanofluid. Nield and Kuznetsov (2011) investigated the cross diffusion in nanofluids. Recently, a boundary layer analysis for the natural convection past a horizontal plate in a porous medium saturated with a nanofluid is analyzed by Gorla and Chamkha (2011). Many problems of magnetohydrodynamics (MHD) flows of porous media (Darcian and non-Darcian) saturated with Newtonian as well as non-Newtonian fluids [see Chamkha and Aly (2010); Hamada et al. (2011)] have been analyzed and reported in the literature due to its importance in the various fields. Some of the authors [e.g., Uddin (2012a); Ferdows et al. (2012)] have explored the importance of MHD in the nanofluids. As has been pointed out by others, magnetic nanofluids have many applications: magnetofluidic leakage-free rotating seals, magnetogravimetric separations acceleration/inclinations sensors, aerodynamic sensors (differential pressure, volumic flow), nano-/micro-structured magnetorheological fluids for semiactive vibration dampers, and biomedical applications in plant genetics and veterinary medicine.

The viscous dissipation effect, that is, a local production of thermal energy through the mechanism of viscous stresses, serves to modify, sometimes greatly, free, forced, and mixed convection flows in both clear viscous fluids and in fluid-saturated porous media. Several researchers (Gebhart, 1962; Takhar and Beg, 1997; Murthy and Singh, 1997; Rees et al., 2003; Nield, 2007) have focused their efforts on the effect of viscous dissipation in porous media in regular fluids/fluid-saturated porous medium, but there is very limited literature available on the study of viscous dissipation in nanofluids about different surface geometries. Uddin et al. (2012b) analyzed the influences of viscous dissipation on the free convective boundary layer flow of a non-Newtonian power-law nanofluid over an isothermal vertical flat plate embedded in a porous medium. The effects of suction, viscous dissipation, thermal radiation, and thermal diffusion numerically studied on a boundary layer flow of nanofluids over a moving flat plate have been discussed by Motsumi and Makinde (2012). Kameswaran et al. (2012) investigated the convective heat and mass transfer in nanofluid flow over a stretching sheet subject to hydromagnetic, viscous dissipation, chemical reaction, and Soret effects.

There is a more common practical situation, where heat transfer occurs at the boundary surface to or from a fluid flowing on the surface at a known temperature and a known heat transfer coefficient, e.g., in heat exchangers, condensers, reboilers, etc. In view of the above said application, the aim of the present paper is to further contribute to this open research field by describing surprising effects of viscous dissipation and MHD on the mechanism of nanoparticles onto a vertical plate in a non-Darcy porous medium saturated with a nanofluid. The implicit, iterative finite-difference method discussed by Blottner (1970) is employed to solve the nonlinear system of this particular problem. The effects of magnetic, viscous dissipation, non-Darcy, and Biot parameters are examined and are displayed through graphs. Based on the author's knowledge, the present model has not been reported in the literature.

2. MATHEMATICAL FORMULATION

Consider the steady two-dimensional free convection flow of an electrically conducting fluid from the vertical flat plate in a nanofluid-saturated non-Darcy porous medium. The coordinate system is chosen such that the x-axis is along the vertical plate and the y-axis is normal to the plate. The physical model and coordinate system are shown in Fig. 1. A uniform magnetic field is applied normal to the plate. The magnetic Reynolds number is assumed to be small so that the induced magnetic field can be neglected. The fluid and the porous structure are everywhere in local thermodynamic equilibrium and the porous medium is assumed to be transparent. The fluid flow is moderate, so the pressure drop is proportional to the linear combination of fluid velocity and the square of velocity (Forchheimer flow model is considered). At this boundary, the temperature T_w, to be determined later, is the result of a convective heating process which is characterized by a temperature T_f and a heat transfer coefficient h_f. The nanoparticle volume fraction ϕ at the wall is ϕ_w. The ambient values, attained as y tends to infinity, of T and ϕ are denoted by T_∞ and ϕ_∞, respectively. In addition, the viscous dissipation and the convective boundary condition are incorporated.

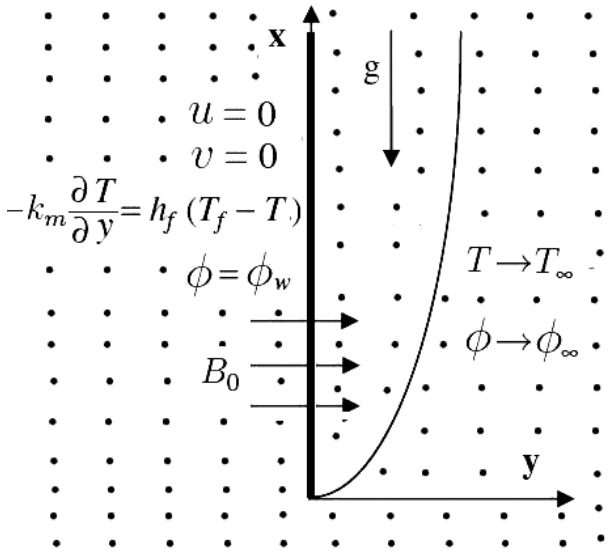

FIG. 1: Physical model and coordinate system.

By employing the Oberbeck-Boussinesq and the standard boundary layer approximations, and making use of the above assumptions and the Darcy-Forchheimer model, the governing equations for the nanofluid flow problem under investigation are given by

$$\frac{\partial u}{\partial x} + \frac{\partial v}{\partial y} = 0, \tag{1}$$

$$\left(1 + \frac{\sigma \mu_e^2 B_0^2 K}{\mu}\right) u + \frac{c\sqrt{K}}{\left(\frac{\mu}{\rho f_\infty}\right)} u^2 = \frac{K(1-\phi_\infty)\rho f_\infty g \beta}{\mu} \times (T - T_\infty) - \frac{(\rho_P - \rho f_\infty) g K}{\mu} (\phi - \phi_\infty), \tag{2}$$

$$u\frac{\partial T}{\partial x} + v\frac{\partial T}{\partial y} = \alpha_m \frac{\partial^2 T}{\partial y^2} + J\left[D_B \frac{\partial \phi}{\partial y}\frac{\partial T}{\partial y} + \frac{D_T}{T_\infty}\left(\frac{\partial T}{\partial y}\right)^2\right] + \frac{\nu}{k_m C_p} u \left[u + \frac{c\sqrt{K}}{\left(\frac{\mu}{\rho f_\infty}\right)} u^2\right], \tag{3}$$

$$\frac{1}{\varphi}\left(u\frac{\partial \phi}{\partial x} + v\frac{\partial \phi}{\partial y}\right) = D_B \frac{\partial^2 \phi}{\partial y^2} + \frac{D_T}{T_\infty}\frac{\partial^2 T}{\partial y^2}, \tag{4}$$

where u and v are the Darcy velocity components in the x and y directions, respectively, T is the temperature, ϕ is the nanoparticle concentration, g is the acceleration due to gravity, K is the permeability, c is the empirical constant associated with the Forchheimer porous inertia term, σ is the electrical conductivity of the fluid, μ_e is the magnetic permeability, B_0 is the strength of the magnetic field, φ is the porosity, $\alpha_m = k_m/(\rho c)_f$ is the thermal diffusivity of the fluid, $\nu = \mu/\rho f_\infty$ is the kinematic viscosity coefficient, and $J = \varphi(\rho c)_p/(\rho c)_f$. Further, ρf_∞ is the density of the base fluid and ρ, μ, k_m, and β are the density, viscosity, thermal conductivity, and volumetric thermal expansion coefficients of the nanofluid, while ρ_p is the density of the nanoparticles, $(\rho c)_f$ is the heat capacity of the fluid, and $(\rho c)_p$ is the effective heat capacity of the nanoparticle material. The coefficients that appear in Eqs. (3) and (4) are the Brownian diffusion coefficient D_B, the thermophoretic diffusion coefficient D_T, and the last term in Eq. (3) is the viscous dissipation term, which can be approximated as the work done by the surface and the body forces acting on the pore [see Murthy and Singh (1997)]. For detailed derivation of Eqs. (1)–(4), one can refer to the papers by Buongiorno (2006) and Nield and Kuznetsov (2009a,b).

The associated boundary conditions are

$$v = 0, \quad -k_m \frac{\partial T}{\partial y} = h_f (T_f - T), \phi = \phi_w \quad \text{at} \quad y = 0, \tag{5a}$$

$$u = 0, \quad T = T_\infty, \quad \phi = \phi_\infty \quad \text{as} \quad y \to \infty, \tag{5b}$$

where the subscripts w and ∞ indicate the conditions at the wall, and at the outer edge of the boundary layer, respectively, where k_m is the thermal conductivity of the fluid.

We introduce the following nondimensional transformations,

$$\eta = \frac{y}{x}\mathrm{Ra}_x^{1/2}, \quad \psi(x,\eta) = \alpha_m \mathrm{Ra}_x^{1/2} f(x,\eta), \quad \theta(x,\eta) = \frac{T - T_\infty}{T_f - T_\infty}, S(x,\eta) = \frac{\phi - \phi_\infty}{\phi_w - \phi_\infty}, \tag{6}$$

where $\mathrm{Ra}_x = [(1-\phi_\infty)\rho f_\infty g K \beta (T_f - T_\infty)x]/[\mu \alpha_m]$ is the local Rayleigh number.

In view of the continuity equation (1), we introduce the stream function ψ by

$$u = \frac{\partial \psi}{\partial y}, \quad v = -\frac{\partial \psi}{\partial x}. \tag{7}$$

Substituting Eq. (7) into Eqs. (2)–(4) and then using the nondimensional transformations (6), we get the following system of nondimensional equations:

$$(1 + \mathrm{Ha}) f' + \mathrm{Gr} f'^2 = \theta - \mathrm{Nr}\, S, \tag{8}$$

$$\theta'' + \frac{1}{2} f\theta' + \mathrm{Nb}\,\theta' S' + \mathrm{Nt}\,\theta'^2 + \varepsilon f'^2 (1 + \mathrm{Gr} f') = \varepsilon \left(f' \frac{\partial \theta}{\partial \varepsilon} - \theta' \frac{\partial f}{\partial \varepsilon} \right), \quad (9)$$

$$S'' + \frac{1}{2} \mathrm{Le}\, f\, S' + \frac{\mathrm{Nt}}{\mathrm{Nb}} \theta'' = \mathrm{Le}\, \varepsilon \left(f' \frac{\partial S}{\partial \varepsilon} - S' \frac{\partial f}{\partial \varepsilon} \right), \quad (10)$$

where the primes indicate partial differentiation with respect to η alone, $\mathrm{Gr} = [(c\sqrt{K})/v][(\alpha_m)/x]\mathrm{Ra}_x$ is the non-Darcy parameter, $\mathrm{Le} = (\alpha_m)/(\varphi D_B)$ is the Lewis number, $\mathrm{Nr} = [(\rho_p - \rho f_\infty)(\phi_w - \phi_\infty)]/[\rho f_\infty \beta (1 - \phi_\infty)(T_f - T_\infty)]$ is the buoyancy parameter, $\mathrm{Nb} = [JD_B(\phi_w - \phi_\infty)]/[\alpha_m]$ is the Brownian motion parameter, $\mathrm{Nt} = [JD_T]/[\alpha_m T_\infty (T_f - T_\infty)]$ is the thermophoresis parameter, $\mathrm{Ha} = (\sigma \mu_e^2 B_0^2 K)/\mu$ is the magnetic field parameter, and $\varepsilon = [(1 - \phi_\infty) g \beta x]/C_p$ is the viscous dissipation parameter (i.e., Eckert number). For most situations the Darcy number is small, so viscous dissipation is important at even modest values of the Eckert number. The circumstances in which viscous dissipation is important are those involving flows of relatively large velocity. The author believes that the results in this paper are likely to be applicable in the context of particle bed nuclear reactors.

The boundary conditions (5) in terms of f, θ, and S become

$$\eta = 0: \quad f(\varepsilon, 0) = -2\varepsilon \frac{\partial f}{\partial \varepsilon}, \quad \theta'(\varepsilon, 0) = -\mathrm{Bi}\varepsilon^{1/2} \times [1 - \theta(\varepsilon, 0)], \quad S(\varepsilon, 0) = 1, \quad (11a)$$

$$\eta \to \infty: \quad f'(\varepsilon, \infty) \to 0, \quad \theta(\varepsilon, \infty) \to 0, \quad S(\varepsilon, \infty) \to 0, \quad (11b)$$

where $\mathrm{Bi} = \{h_f/k_m\}\{\sqrt{[C_p x]/[(1 - \phi_\infty) g \beta \mathrm{Ra}_x]}\}$ is the Biot number. It is important to note that as the convective parameter Bi increases, the heat transfer rates approaches the isothermal case. This statement is also supported by the first thermal boundary condition of Eq. (11a), which gives $\theta(\varepsilon, 0) = 1$ as $\mathrm{Bi} \to \infty$.

If $\varepsilon = 0$, $\mathrm{Ha} = 0$, and $\mathrm{Gr} = 0$, the problem reduces to natural convective boundary-layer flow in a porous medium saturated by a nanofluid under convective boundary condition. In the limit $\varepsilon \to 0$, the governing equations (8)–(10) reduce to the corresponding equations for a non-Darcy porous medium saturated with nanofluid under convective boundary condition in the presence of MHD effects. Furthermore, if $\mathrm{Bi} \to \infty$, $\mathrm{Nb} \to 0$, $\mathrm{Nt} = \mathrm{Nr} = 0$, $\varepsilon = 0$, $\mathrm{Ha} = 0$, and $S(\eta) \to 0$ (i.e., for the regular Newtonian fluid), and with the choice of boundary condition at $\eta = 0$: $f = 0$, $\theta = 1$, Eqs. (8)–(10) governing the non-Darcy porous medium saturated with a nanofluid reduce to the non-Darcy natural convection from vertical isothermal surfaces in saturated porous media in the absence of viscous dissipation and MHD effects.

3. HEAT AND MASS TRANSFER COEFFICIENTS

The primary objective of this study is to estimate the parameters of engineering interest in fluid flow, heat, and mass transport problems, which are the Nusselt number Nu_x, and nanoparticle Sherwood number Sh_x. These parameters characterize the wall heat and nanoparticle mass transfer rates, respectively.

The local heat and local nanoparticle mass fluxes from the vertical plate can be obtained from

$$q_w = -k_m \left(\frac{\partial T}{\partial y} \right)_{y=0}, \quad q_m = -D_B \left(\frac{\partial \phi}{\partial y} \right)_{y=0}. \quad (12)$$

The dimensionless local Nusselt number $\mathrm{Nu}_x = [q_w x]/[k_m (T_f - T_\infty)]$ and local nanoparticle Sherwood number $\mathrm{Sh}_x = [q_m x]/[D_B(\phi_w - \phi_\infty)]$ are given by

$$\frac{\mathrm{Nu}_x}{\mathrm{Ra}_x^{1/2}} = -\theta'(\varepsilon, 0) \quad \text{and} \quad \frac{\mathrm{Sh}_x}{\mathrm{Ra}_x^{1/2}} = -S'(\varepsilon, 0). \quad (13)$$

The effects of the various parameters involved in the investigation on these coefficients are discussed in the Results and Discussion section.

4. NUMERICAL METHOD

Equations (8)–(10) represent an initial-value problem with ε playing the role of time. This general nonlinear problem cannot be solved in closed form and, therefore, a numerical solution is necessary to describe the physics of the problem. The implicit, tridiagonal finite-difference method similar to that discussed by Blottner (1970) has proven to be adequate and sufficiently accurate for the solution of this kind of problem. Therefore, it is adopted in the present work. All first-order derivatives with respect to ε are replaced by a two-point backward-difference formula when marching in the positive ε direction. Then, all second-order differential equations in η are discretized using three-point central difference quotients. This discretization process produces a tridiagonal set of algebraic equations at each line of constant ε which is readily solved by the well known Thomas algorithm [see Blottner (1970)]. During the solution, iteration is employed to

deal with the nonlinearity aspect of the governing differential equations. The problem is solved line by line starting with line $\varepsilon = 0$ where similarity equations are solved to obtain the initial profiles of velocity, temperature, and nanoparticles volume fraction and marching forward in ε until the desired line of constant ε is reached. The initial step size $\Delta\eta_1$ and the growth factor K^* employed such that $\Delta\eta_{i+1} = K^*\Delta\eta_i$ (where the subscript i indicates the grid location) were 10^{-3} and 1.0375, respectively, and constant step sizes in the ε direction with $\Delta\varepsilon = 0.01$ are employed. These values were found (by performing many numerical experimentations) to give accurate and grid-independent solutions. The solution convergence criterion employed in the present work was based on the difference between the values of the dependent variables at the current and the previous iterations. When this difference reached 10^{-5}, the solution was assumed converged and the iteration process was terminated.

With Bi $\to \infty$, Nb $\to 0$, Nt $=$ Nr $= 0$, $\varepsilon = 0$, Ha $= 0$, and $S(\eta) \to 0$ (i.e., for the regular Newtonian fluid), and with the choice of boundary condition at $\eta = 0$: $f = 0$, $\theta = 1$, Eqs. (8)–(10) governing the present investigation of nanofluid-saturated non-Darcy porous medium (with isothermal boundary) reduce to those limiting cases of free convection flow. Plumb and Huenefeld (1981) investigated non-Darcy natural convection from vertical isothermal surfaces in saturated porous media in the absence of viscous dissipation and MHD effects. Also, the results have been compared with Plumb and Huenefeld (1981) and it is found that they are in good agreement as shown in Table 1. Therefore, the developed code can be used with great confidence to study the problem considered in this paper.

5. RESULTS AND DISCUSSION

We have computed the solutions for the dimensionless velocity, temperature, and nanoparticle volume fraction functions and heat and nanoparticle mass transfer rates as shown graphically in Figs. 2–13. The effects of viscous dissipation parameter ε, magnetic parameter Ha, non-Darcy parameter Gr, Biot number Bi, Brownian motion parameter Nb, thermophoresis parameter Nt, Lewis number Le, and buoyancy ration Nr have been discussed.

The dimensionless velocity distribution for different values of Forchheimer number Gr and Biot number Bi with the fixed values of other parameters is depicted in Fig. 2(a). Since Gr represents the inertial drag, thus an increase in the Forchheimer number increases the resistance to the flow and so a decrease in the fluid velocity ensues. Here Gr $= 0$ represents the case where the flow is Darcian. The velocity is maximum in this case due to the total absence of inertial drag. The reverse trend can be seen in the case of convective parameter Bi. The dimensionless temperature for different values of Forchheimer number Gr Biot number Bi for the fixed values of other parameters is displayed in Fig. 2(b). An increase in Forchheimer number Gr increases temperature values, since as the fluid is decelerated, energy is dissipated as heat and serves to increase temperatures. As such the temperature is minimized for the lowest value of Gr and maximized for the highest value of Gr as shown in Fig. 2(b). Given that convective heating increases with Biot number, Bi $\to \infty$ simulates the isothermal surface, shown in Fig. 2(b), where $\theta(\varepsilon, 0) = 1 - \varepsilon$ as Bi $\to \infty$. In fact, a high Biot number indicates that the internal thermal resistance of the plate is higher than the boundary layer thermal resistance. As a

TABLE 1: Comparison of dimensionless similarity functions $\theta'(\eta)$ and $f'(\eta)$ for free convection along a vertical flat plate in non-Darcy porous medium with Bi $\to \infty$, Nb $\to 0$, Nt $=$ Nr $= 0$, $\varepsilon = 0$, Ha $= 0$, and $S(\eta) \to 0$; with boundary conditions $\eta = 0$: $f = 0$, $\theta = 1$ (Plumb and Huenefeld, 1981)

	$\theta'(0)$		$f'(0)$	
Gr	**Plumb and Huenefeld (1981)**	**Present**	**Plumb and Huenefeld (1981)**	**Present**
0.00	0.44390	0.44374	1.00000	1.00000
0.01	0.44232	0.44216	0.99020	0.99019
0.10	0.42969	0.42950	0.91608	0.91608
1.00	0.36617	0.36575	0.61803	0.61803
10.00	0.25126	0.25065	0.27016	0.27016
100.00	0.15186	0.15145	0.09512	0.09512

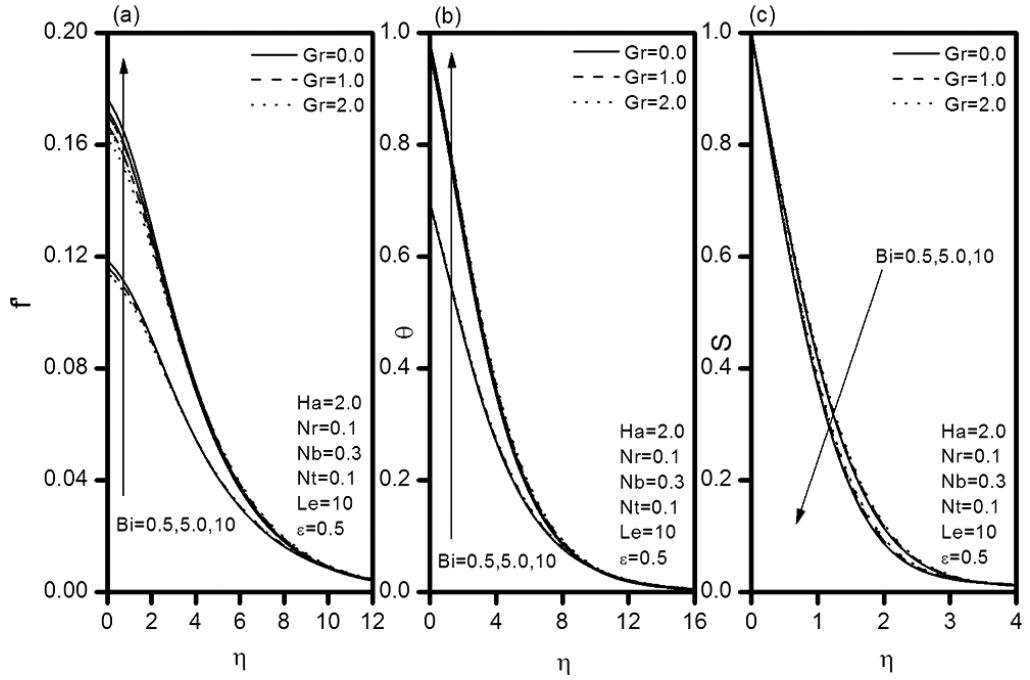

FIG. 2: Effects of non-Darcy parameter and Biot number on (**a**) velocity, (**b**) temperature, and (**c**) volume fraction.

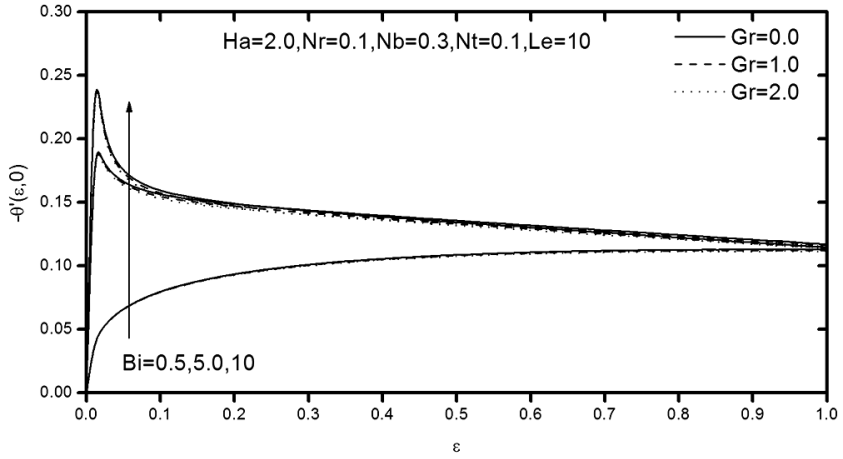

FIG. 3: Variation of nondimensional heat transfer coefficient with ε for different values of non-Darcy parameter and Biot number and fixed values of other parameters.

result, these figures illustrate that an increase in the Biot number leads to increase of fluid temperature, efficiently. Figure 2(c) depicts the dimensionless volume fraction for different values of Forchheimer number Gr and Biot number Bi for fixed values of other parameters. As the parameter Gr increases, the volume fraction profile increases but the opposite behavior can be seen in the case of Bi for the specified conditions. The increase in non-Darcy parameter reduces the intensity of the flow but enhances the thermal and nanoparticle volume fraction boundary layer thicknesses.

In Fig. 3, the nondimensional heat transfer coefficient is plotted against the viscous dissipation parameter ε for different values of Forchheimer number Gr and Biot num-

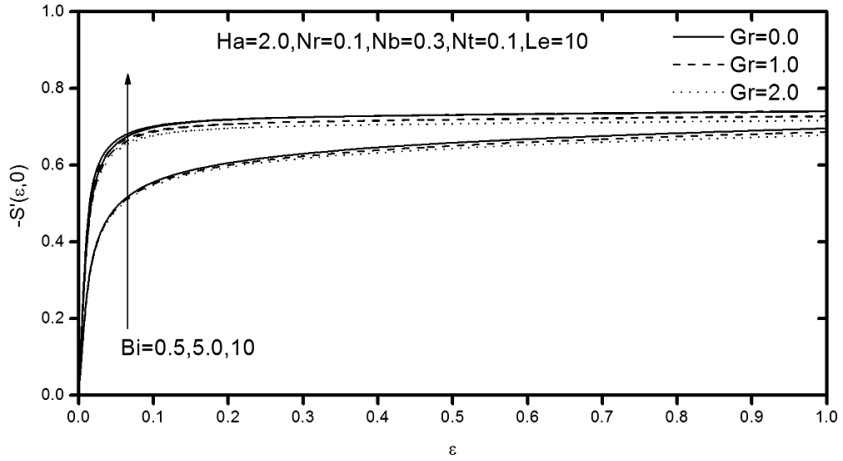

FIG. 4: Variation of nondimensional nanoparticle mass transfer coefficient with ε for different values of non-Darcy parameter and Biot number and fixed values of other parameters.

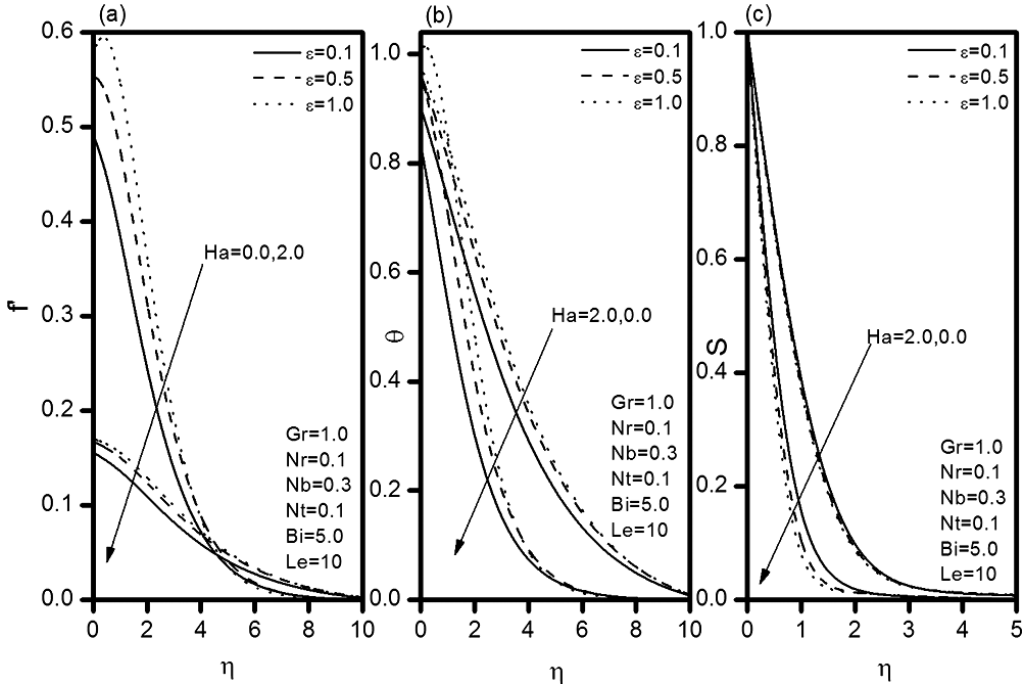

FIG. 5: Effects of viscous dissipation parameter and magnetic parameter on (**a**) velocity, (**b**) temperature, and (**c**) volume fraction.

ber Bi. It indicates that heat transfer rate decreases with the viscous dissipation parameter. Also, the results indicated that increases in Gr decrease the heat transfer coefficient but the reverse phenomena can be observed with the increasing values of Bi.The nondimensional mass transfer coefficient is plotted against the viscous dissipation parameter ε for different Forchheimer number Gr and Biot number Bi in Fig. 4. It is evident from this figure that for increasing values of Gr the nondimensional mass transfer coefficient decreases whereas with increasing values of

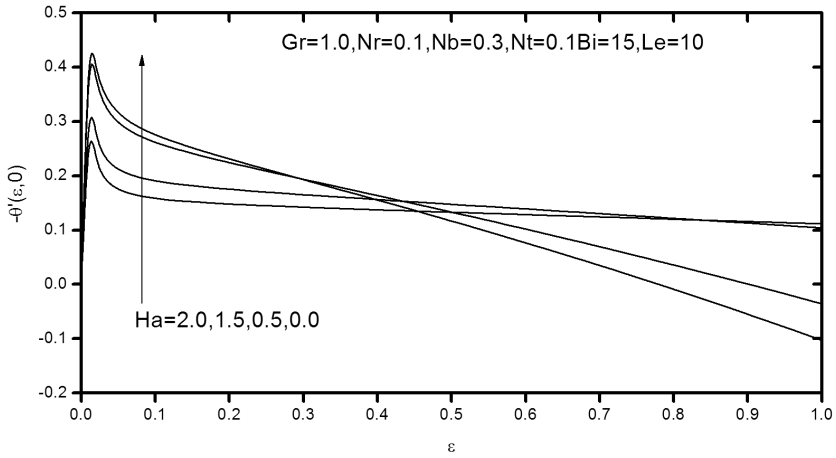

FIG. 6: Variation of nondimensional heat transfer coefficient versus ε for different values of magnetic parameter with fixed values of other parameters.

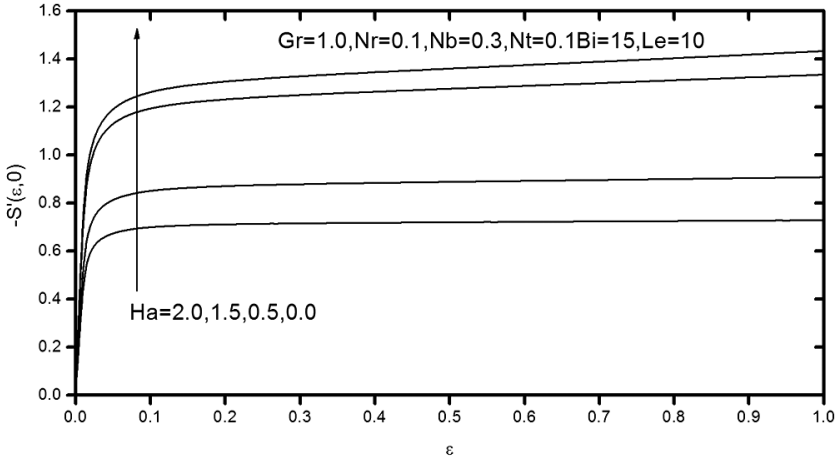

FIG. 7: Variation of nondimensional nanoparticle mass coefficient versus ε for different values of magnetic parameter with fixed values of other parameters.

Bi the nondimensional mass transfer coefficient increases. Finally, the nondimensional mass transfer coefficient increases with increasing values of ε. Hence the non-Darcy parameter has an important role in controlling the flow field.

The variation of the nondimensional velocity, temperature, and nanoparticle concentration for Gr = 1.0, Nr = 0.1, Nb = 0.3, Nt = 0.1, Bi = 5.0, and Le = 10 with magnetic parameter Ha and viscous dissipation parameter (i.e., Eckert number) ε are shown in Fig. 5. It can be observed from Fig. 5(a) that the velocity of the fluid is decreased with increase in the value of the magnetic parameter. This is due to the fact that the introduction of a transverse magnetic field, normal to the flow direction, has a tendency to create the drag known as the Lorentz force which tends to resist the flow. Hence, the horizontal velocity profiles decrease as the magnetic parameter Ha increases. It can be found from Fig. 5(b) that increases in the value of the magnetic parameter increase the temperature of the fluid in the medium. It can be seen from Fig. 5(c) that the nanoparticle volume fraction of the fluid is increased by increasing the value of the magnetic parameter. As explained above, the transverse magnetic field gives rise to a resistive force known as the Lorentz force of an electrically conducting fluid. This force makes the fluid experience resistance by increasing the friction

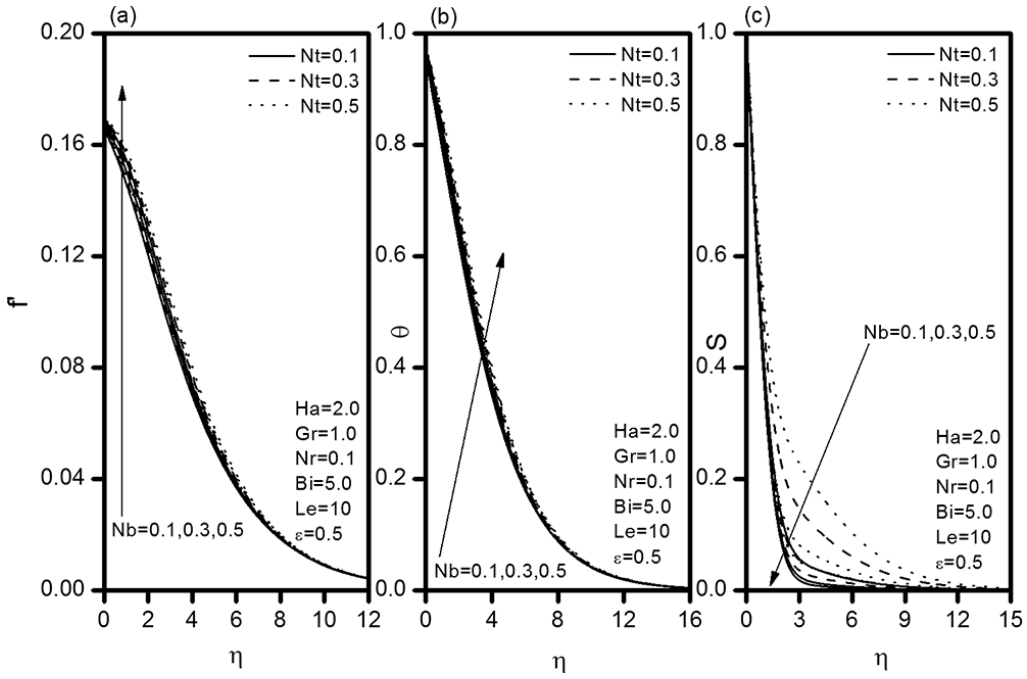

FIG. 8: Effects of Brownian motion and thermophoresis parameters on (**a**) velocity, (**b**) temperature, and (**c**) volume fraction.

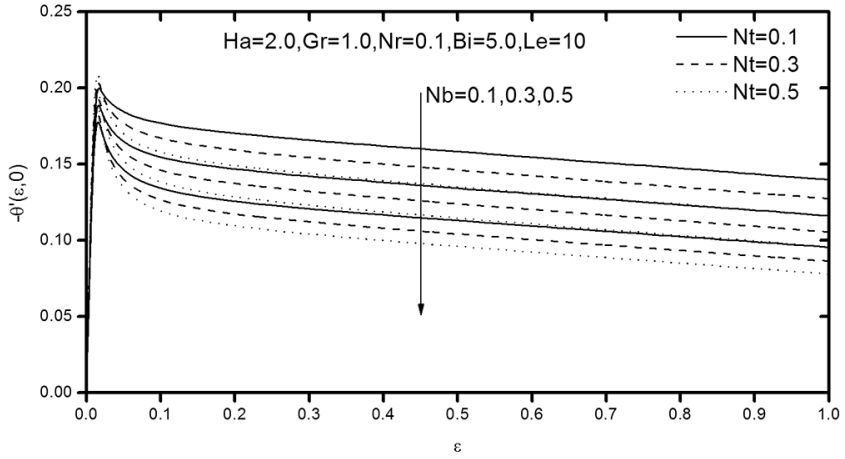

FIG. 9: Variation of nondimensional heat transfer coefficient versus ε for different values of Brownian motion and thermophoresis parameters with fixed values of other parameters.

between its layers and thus increases its temperature and nanoparticle volume fraction. To increase the fluid motion we have considered the viscous dissipation term. From this term we obtained dimensionless parameter ε. This parameter is called the fluid motion controlling parameter. It may be noted that $\varepsilon = 0$ corresponds to the case of the absence of viscous dissipation. Figure 5(a) shows that the velocity field increases with the increase of Eckert number ε. The effect of viscous dissipation ε is to increase the temperature in the boundary layer, which is displayed in Fig. 5(b). Figure 5(c) shows that the concentration field decreases with the increase of Eckert number ε, because

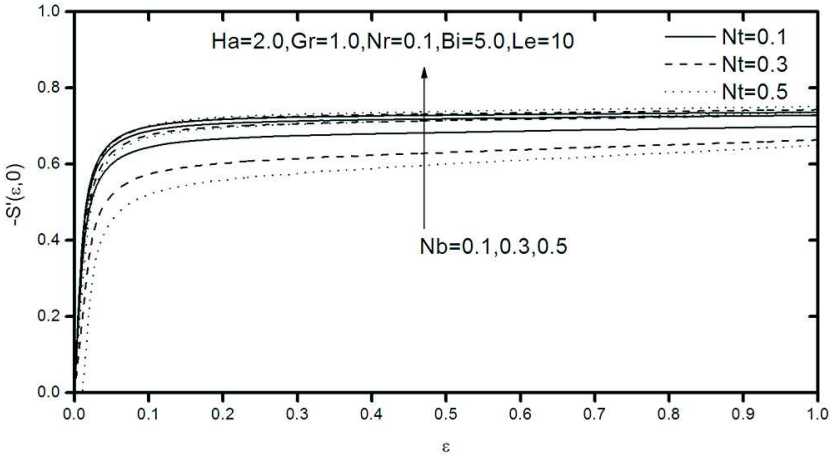

FIG. 10: Variation of nondimensional nanoparticle mass transfer coefficient versus ε for different values of Brownian motion and thermophoresis parameters with fixed values of other parameters.

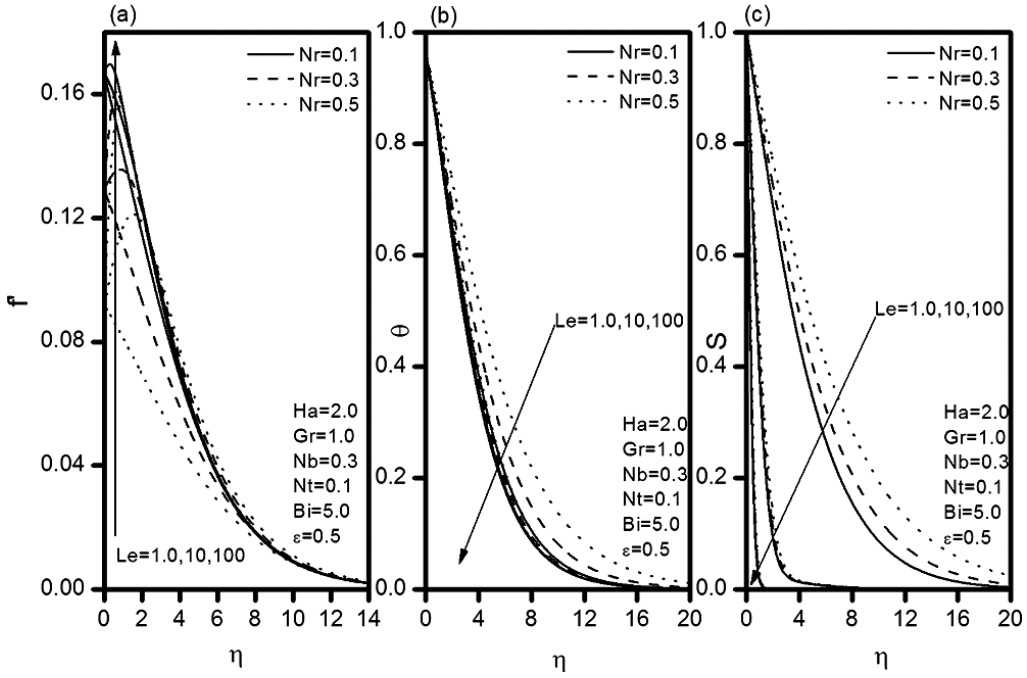

FIG. 11: Effects of nanoparticle buoyancy ratio and Lewis number on (**a**) velocity, (**b**) temperature, and (**c**) volume fraction.

the effect of viscous dissipation in the energy equation acts as an internal distributed heat source generated due to the action of viscous stresses. Therefore, the velocity and temperature distributions are at a higher level when this effect is considered ($\varepsilon \neq 0$) than when this effect is neglected ($\varepsilon = 0$).

The effects of a magnetic field and viscous dissipation on the wall heat and mass transfer rates are shown in Figs. 6 and 7. The influence of a magnetic field is to reduce both the wall heat and mass transfer rates. The viscous dissipation effect reduces the wall heat transfer rate and enhances the wall mass transfer rate. The combined

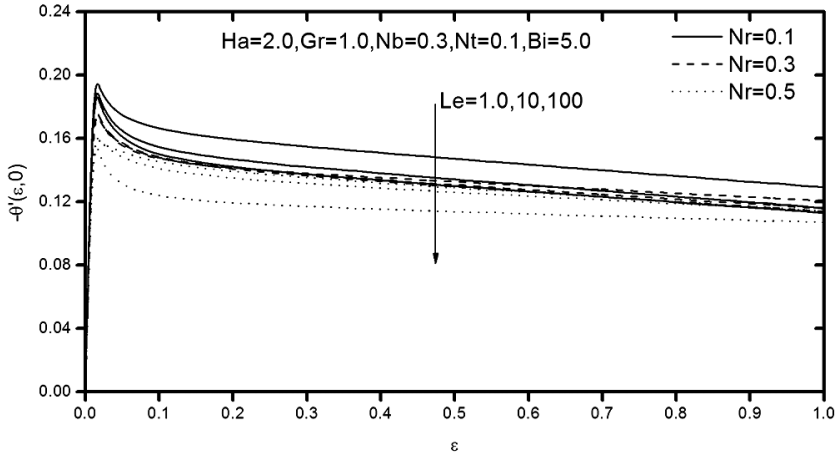

FIG. 12: Variation of nondimensional heat transfer coefficient versus ε for different values of nanoparticle buoyancy ratio and Lewis number with fixed values of other parameters.

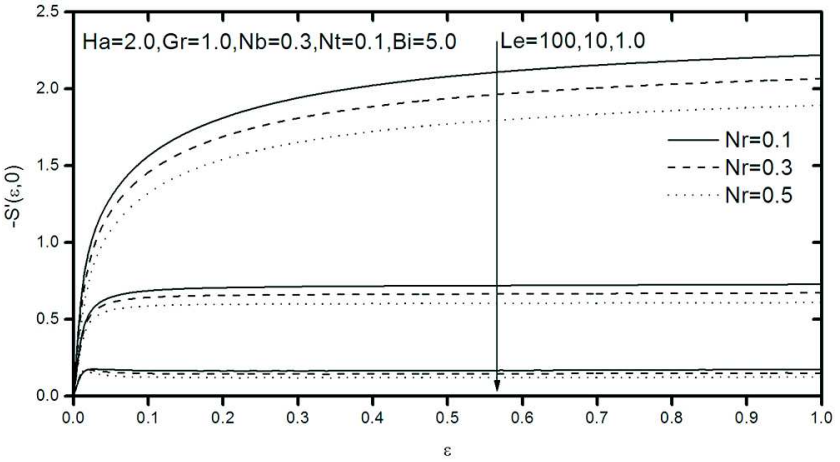

FIG. 13: Variation of nondimensional nanoparticle mass transfer coefficient versus ε for different values of nanoparticle buoyancy ratio and Lewis number with fixed values of other parameters.

effect of the magnetic field and the viscous dissipation (see Fig. 5) is to generate more heat in the boundary layer region and hence to reduce the wall heat transfer rate.

Figure 8 is prepared to present the effect of the Brownian motion Nb and thermophoresis Nt on the velocity, temperature, and volume fraction distributions. With $\mathrm{Nb} = 0$, there is no thermal transport due to buoyancy effects created as a result of nanoparticle concentration gradients. It is observed that the momentum boundary layer thickness increases with the increase of Nb and Nt. As the parameters Nt and Nb increase, the temperature increases for the specified conditions. As expected, the boundary layer profile for the temperature function is essentially the same form as in the case of a regular (Newtonian) fluid. The nanoparticle volume fraction decreases with increase in Nb but increases with Nt. It is noticed that the nanoparticle volume fraction increases with increase in Nb in the case of forced convection flow. We notice that positive Nt indicates a cold surface, while negative indicates a hot surface. For hot surfaces, thermophoresis tends to blow the nanoparticle volume fraction boundary layer away from the surface since a hot surface repels the submicron-sized particles from it, thereby forming a relatively particle-free layer near the surface.

The nondimensional heat transfer coefficient decreases with increasing values of stratification parameter as well as with Brownian motion and thermophoresis parameters as shown in Fig. 9. As ε increases, it can be observed from Fig. 9 that the maximum of nondimensional heat transfer rate decreases in amplitude. Further, it can be seen that the values of nondimensional mass transfer coefficient increase with an increase in both viscous dissipation parameter and Brownian motion but the reverse trend can be seen from Fig. 10 with the thermophoresis parameter.

The variation of the nondimensional velocity, temperature, and nanoparticle concentration for Ha $= 2.0$, Gr $= 1.0$, Nb $= 0.3$, Nt $= 0.1$, Bi $= 0.5$, and $\varepsilon = 0.5$ with Lewis number Le and nanoparticle buoyancy ratio Nr is shown in Fig. 11. It is noticed from Fig. 11 that an increase in the Lewis number Le results in an increase in the velocity but a decrease in the temperature and volume fraction within the boundary layer. The present analysis shows that the flow field is appreciably influenced by the Lewis number Le. As nanoparticle buoyancy ratio Nr increases, it can be observed from Fig. 11(a) that the maximum velocity decreases in amplitude. The location of the maximum velocity moves farther away from the wall. It is clearly seen from Figs. 11(b) and 11(c) that increase in Nr tends to increase the thermal and nanoparticle volume fraction boundary layer thickness.

The nondimensional heat transfer coefficient is plotted against the viscous dissipation parameter ε in Fig. 12 for different values of nanoparticle buoyancy ratio Nr and Lewis number Le. It indicates that heat transfer rate decreases with the increasing values of Nr and Le. In Fig. 13, the nondimensional mass transfer coefficient is plotted against the viscous dissipation parameter ε for different nanoparticle buoyancy ratio Nr and Lewis number Le. It is evident from this figure that for increasing values of Nr and Le, the nondimensional mass transfer coefficient decreases. Finally, the nondimensional heat transfer rate decreases but nanoparticle mass transfer rate increases with increasing values of ε.

6. CONCLUSION

In this paper, we studied the effect of viscous dissipation and magnetic field on free convection in a non-Darcy porous medium saturated with nanofluid under convective boundary condition. Using the dimensionless variables, the governing equations were transformed into a set of nonlinear parabolic equations where numerical solution was presented using the implicit, iterative finite-difference method discussed by Blottner (1970) for a wide range of parameters. The following conclusions were obtained:

- Increasing the magnetic field parameter Ha resulted in lower velocity distribution and heat and nanoparticle mass transfer rate but higher temperature and nanoparticle volume fraction distributions in the boundary layer.
- An increase in the non-Darcy parameter Gr produced decreases in the velocity distribution, heat and nanoparticle mass transfer rates, and increases in the temperature and nanoparticle volume fraction distributions.
- An increase in the viscous dissipation parameter ε caused increases in the velocity and temperature distribution, nanoparticle mass transfer rate, and decreases in the nanoparticle volume fraction distribution and the heat transfer rate.
- An increase in the Brownian motion parameter Nb, enhanced the velocity and temperature distributions and the nanoparticle mass transfer rate but reduced the nanoparticle volume fraction and heat transfer rate in the boundary layer.
- An increase in the thermophoresis parameter Nt resulted in increases in the velocity, temperature, and the nanoparticle volume fraction distributions, but decreases in the nondimensional heat and nanoparticle mass transfer rates in the boundary layer.
- An increase in the Lewis number Le produced reductions in the temperature and the nanoparticle volume fraction distributions and increases in the velocity, heat transfer rate, and the nanoparticle mass transfer rate in the boundary layer.
- An increase in the Biot number Bi caused enhancements in the velocity, temperature, and the nondimensional heat and nanoparticle mass transfer rates, whereas it caused a reduction in the nanoparticle volume fraction in the boundary layer.
- An increase in the nanoparticle buoyancy parameter Nr produced a reduction in the velocity near the wall and an opposite behavior far away from the wall distribution. Also, the temperature and nanoparticle volume fraction distributions increased but the heat and nanoparticle mass transfer rates decreased with increases in the value of Nr.

- The results also indicated that the presence of MHD and viscous dissipation effects in the nanofluid-saturated non-Darcy porous medium influenced the flow, heat, and the nanoparticle volume fraction significantly.

REFERENCES

Blottner, F. G., Finite-difference methods of solution of the boundary layer equations, *AIAA. J.*, vol. **8**, pp. 193–205, 1970.

Buongiorno, J., Convective transport in nanofluids, *ASME J. Heat Transfer*, vol. **128**, pp. 240–250, 2006.

Chamkha, A. J. and Aly, A. M., MHD free convection flow of a nanofluid past a vertical plate in the presence of heat generation or absorption effects, *Chem. Eng. Commun.*, vol. **198**, pp. 425–441, 2010.

Chamkha, A. J., Gorla, R. S. R., and Ghodeswar, K., Non-similar solution for natural convective boundary layer flow over a sphere embedded in a porous medium saturated with a nanofluid, *Transp. Porous Media*, vol. **86**, pp. 13–22, 2011.

Choi, S. U. S., Enhancing thermal conductivity of fluid with nanoparticles, In Siginer, D. A. and Wang, H. P., eds., *Developments and Applications of Non-Newtonian Flows: Proceedings of the ASME International Mechanical Engineering Congress and Exposition, 1995, San Francisco, CA*, New York: ASME, pp. 99–105, 1995.

Das, S. K., Choi, S. U. S., Yu, W., and Pradeep, T., *Nanofluids: Science and Technology*, Hoboken, NJ: Wiley 2007.

Ferdows, M., Shakhaoath Khan, Md., Mahmud Alam, Md., and Shuyu, S., MHD mixed convective boundary layer flow of a nanofluid through a porous medium due to an exponentially stretching sheet, *Math. Probl. Eng.*, Article ID 408528, vol. **2012**, pp. 1–21, 2012.

Gebhart, B., Effects of viscous dissipation in natural convection, *J. Fluid Mech.*, vol. **14**, pp. 225–232, 1962.

Gorla, R. S. R. and Chamkha, A. J., Natural convective boundary layer flow over a horizontal plate embedded in a porous medium saturated with a nanofluid, *J. Mod. Phys.*, vol. **2**, pp. 62–71, 2011.

Hamada, M. A. A., Pop, I., and Md. Ismail, A. I., Magnetic field effects on free convection flow of a nanofluid past a vertical semi-infinite flat plate, *Nonlinear Anal.: Real World Appl.*, vol. **12**, pp. 1338–1346, 2011.

Kakac, S. and Pramuanjaroenkij, A., Review of convective heat transfer enhancement with nanofluids, *Int. J. Heat Mass Transfer*, vol. **52**, pp. 3187–3196, 2009.

Kameswaran, P. K., Narayana, M., Sibanda, P., and Murthy, P. V. S. N., Hydro-magnetic nanofluid flow due to a stretching or shrinking sheet with viscous dissipation and chemical reaction effects, *Int. J. Heat Mass Transfer*, vol. **55**, pp. 7587–7595, 2012.

Motsumi, T. G. and Makinde, O. D., Effects of thermal radiation and viscous dissipation on boundary layer flow of nanofluids over a permeable moving flat plate, *Phys. Scr.*, vol. **86**, p. 045003, 2012.

Murthy, P. V. S. N. and Singh, P., Effect of viscous dissipation on a non-Darcy natural convection regime, *Int. J. Heat Mass Transfer*, vol. **40**, pp. 1251–1260, 1997.

Nield, D. A., The modeling of viscous dissipation in a saturated porous medium, *J. Heat Transfer*, vol. **129**, pp. 1459–1463, 2007.

Nield, D. A. and Kuznetsov, A. V., The Cheng-Minkowycz problem for natural convective boundary-layer flow in a porous medium saturated by a nanofluid, *Int. J. Heat Mass Transfer*, vol. **52**, pp. 5792–5795, 2009a.

Nield, D. A. and Kuznetsov, A. V., Thermal instability in a porous medium layer saturated by a nanofluid, *Int. J. Heat Mass Transfer*, vol. **52**, pp. 5796–5801, 2009b.

Nield, D. A. and Kuznetsov, A. V., The Cheng-Minkowycz problem for the double-diffusive natural convective boundary layer flow in a porous medium saturated by a nanofluid, *Int. J. Heat Mass Transfer*, vol. **54**, pp. 374–378, 2011.

Plumb, O. A. and Huenefeld, J. C., Non-Darcy natural convection from heated surfaces in saturated porous media, *Int. J. Heat Mass Transfer*, vol. **24**, pp. 765–768, 1981.

Rees, D. A. S., Magyari, E., and Keller, B., The development of the asymptotic viscous dissipation profile in a vertical free convective boundary layer flow in a porous medium, *Transp. Porous Media*, vol. **53**, pp. 347–355, 2003.

Takhar, H. G. and Beg, O. A., Effects of transverse magnetic field, Prandtl number and Reynolds number on non-Darcy mixed convective flow of an incompressible viscous fluid past a porous vertical flat plate in a saturated porous medium, *Int. J. Energy Res.*, vol. **21**, pp. 87–100, 1997.

Uddin, M. J., Khan, W. A., and Ismail, A. I., MHD free convective boundary layer flow of a nanofluid past a flat vertical plate with Newtonian heating boundary condition, *PLoS One*, vol. **7**, p. e49499, 2012a.

Uddin, M. J., Khan, W. A., and Ismail, A. I., Effect of dissipation on free convective flow of a non-Newtonian nanofluid in a porous medium with gyrotactic microorganisms, *Proc. Inst. Mech. Eng., Part NNanoengineering and Nanosystems*, vol. **227**, pp. 1–8, 2012b.